nature photonics
LETTERS
PUBLISHED ONLINE: XX XX 2011 | DOI: 10.1038/NPHOTON.2011.217

The mode-locking transition of random lasers

Marco Leonetti[1], Claudio Conti[2] and Cefe Lopez[1]*

The discovery of the spontaneous mode-locking of lasers[1,2], that is, the synchronous oscillation of electromagnetic modes in a cavity, has been a milestone of photonics allowing the realization of oscillators delivering ultrashort pulses. This process is so far known to occur only in standard ordered lasers and only in the presence of a specific device (the saturable absorber). By engineering a mode-selective pumping mechanism we show that it is possible to continuously drive a random laser[3] composed of micrometre-sized laser resonances dwelling in intrinsically disordered, self-assembled clusters of nanometre-sized particles, from a configuration in which the various excited electromagnetic modes oscillate in the form of several, weakly interacting resonances[4,5] to a collective Q1 **strongly interacting regime[6,7]. This phenomenon, which opens the way to the development of a new generation of miniaturized and all-optically controlled light sources, may be explained as the first evidence of spontaneous mode-locking in disordered resonators.**

Random lasers (RLs) are made from disordered highly scattering materials that are able to amplify light when pumped externally. The simultaneous presence of structural disorder and nonlinearity makes these devices particularly promising for connecting photonics with advanced theoretical paradigms[8] such as chaos[9], non-Gaussian statistics[10], complexity[11] and also the physics of Bose–Einstein condensation[12]. Historically, there has been a breach in Q2 RL interpretation. In pioneering experiments, a smooth, single-peaked emission was produced by pumping finely ground laser crystals[13] or titania particles dispersed in a dye-doped solution[7]. This phenomenon has been dubbed RL with incoherent feedback (IFRL), because it may be explained in the framework of the diffusion approximation[14], which neglects interference and treats light rays as trajectories of random walking particles. However, this theoretical framework does not explain another kind of RL that exhibits sub-nanometre sharp spectral peaks[15] associated with high-*Q* resonances[16–19], known as resonant feedback random laser (RFRL).

Standard multimode lasers without disorder and characterized by equispaced resonances may be driven to a synchronous regime through the so-called mode-locking transition, which so far has only been shown to occur spontaneously in the presence of a saturable absorber and allows the generation of ultrashort light pulses[20,21]. We show that the same transition occurs in RLs, allowing us to lock the modes of an RFRL, casting its emission in the typical IFRL spectrum and demonstrating the inherently coherent nature of the random lasing phenomenon.

The system we consider here comprises an isolated micrometre-sized cluster of titania nanoparticles with static disorder, immersed in a rhodamine dye solution (see Supplementary Information). Selected areas surrounding the cluster are pumped optically to generate a directional stimulated emission from the population-inverted areas defined by shaping the beam of a solid-state pump laser using Q3 a reflective spatial light modulator.

Figure 1a presents spiky spectra (RFRL) obtained by averaging over 100 pump pulses ('shots') and collecting light emitted off-plane from the centre of a cluster illuminated by stripe-shaped, directional pumping (see Methods). Notably, the spectral position of the peaks remains unchanged from shot to shot. Dashed and continuous black lines in Fig. 1a correspond to stripes differing by a rotation of 15° (see insets). Similar results are obtained for a stripe with twice the width (red line in Fig. 1a), whereas changing the stripe orientation activates different sets of modes, as revealed by a change in the peaks' positions. Figure 1c–e shows the spatial intensity distribution corresponding to the averaged spectra in Fig. 1a. Figure 1c,e corresponds to different stripe orientations and displays uncorrelated intensity distributions. All the spots in Fig. 1e are also present in Fig. 1d, which corresponds to a stripe with larger width but identical orientation (red and black continuous lines in Fig. 1a). The stripe orientation therefore affects the spatial distribution of the intensity and selects the set of activated

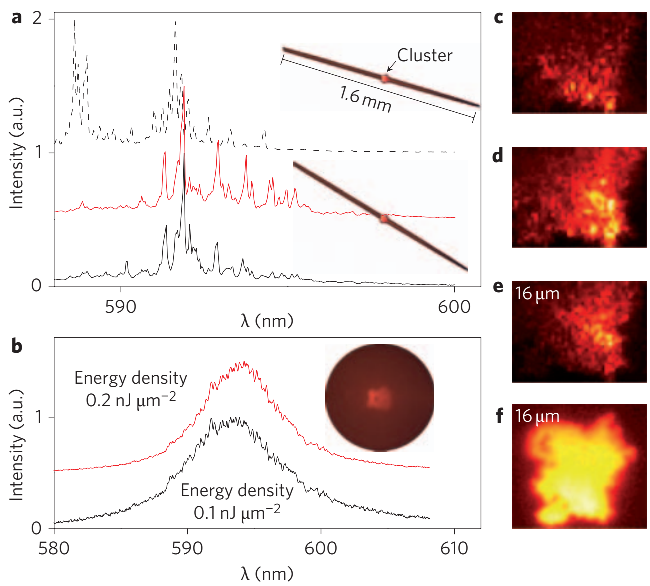

Figure 1 | The two random lasing regimes. **a**, Three normalized spectra, each obtained by averaging 100 single shots from pumping a stripe-shaped area (length, 1.6 mm). Top and bottom traces were retrieved for a stripe of the same thickness (16 μm), but with different orientations (15° tilt). The middle trace is for a stripe with the same orientation as for the bottom trace, but with twice the thickness. **b**, Spectrum for disk-shaped pumping (diameter, 1 mm) for two different pump densities. The insets show sketches of the pumping areas. **c**–**f**, Emitted intensity distributions corresponding to the lines in **a** and **b**. Images were retrieved by optical imaging of the RL emission obtained with a pumping fluence of 0.1 nJ μm^{-2}. Scale bars, 16 μm. Q12

[1]Instituto de Ciencia de Materiales de Madrid (CSIC) and Unidad Asociada CSIC-UVigo, Calle Sor Juana Inés de la Cruz 3, 28049 Madrid, Spain, [2]Dep. Molecular Medicine and CNR-ISC Dep. Physics, University Sapienza, P.le Aldo Moro 5, I-00185, Rome, Italy. *e-mail: cefe@icmm.csic.es

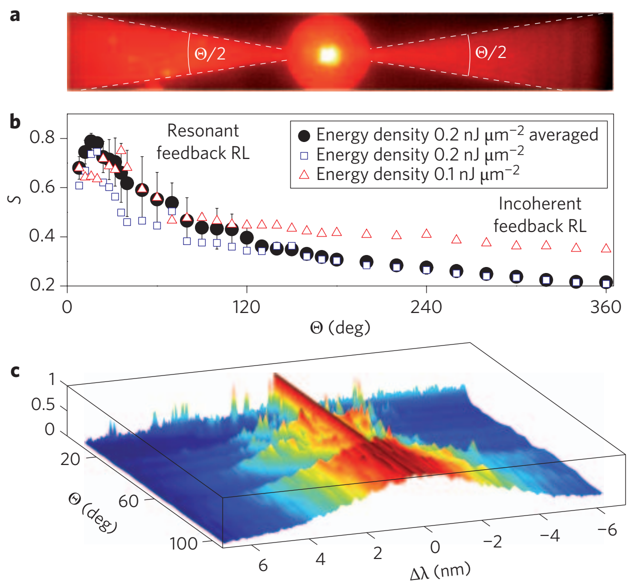

Figure 2 | From spiky to smooth RL spectra. a, Cluster and surrounding pumped area for $\Theta = 36°$. **b**, S as a function of Θ. Squares and triangles correspond to different pump energies for cluster C1. Filled circles correspond to the average of five measurements from different clusters. Error bars indicate standard deviation. **c**, Three-dimensional graph showing normalized spectra (average over 100 shots with a fluence of 0.2 nJ μm^{-2}), for different Θ. Spectra are arbitrarily shifted in frequency to superimpose intensity maxima. $\Delta\lambda$ is the wavelength shift from the
Q13 most intense peak.

modes. Figure 1b shows the measured spectra when the cluster (sample C1) is placed in the centre of a circular pump spot (diameter, 1 mm) and no directionality is present. In this configuration, the spectra are smooth (IFRL) and narrow when the energy is increasing, and the spatial intensity is homogeneously distributed Q4 (Fig. 1f). Having established that we can selectively excite different modes, we proceed to study the effect of the geometry of the pump spot on the RL emission properties.

To study the transition from RFRL to IFRL we engineered a more complex pumping design (consisting of a small circle and two wedges), in which the effective input directions are controlled by parameter Θ (see Methods and Fig. 2a). Spectra observed for small Θ ($\sim$10°) display several very narrow ($\sim$0.05 nm) peaks, whereas large values of Θ ($\sim$100°) produce a single and smooth RL lineshape ($\sim$4 nm).

To classify a RL into IFRL or RFRL categories, we measure its spi- Q5 kiness, S, that is, the amount of high-frequency components in the spectrum (see Methods). Figure 2b is a plot of S versus Θ at different pump energies for sample C1 (squares and triangles) and averaged over five different clusters (filled circles). All curves display the same trend, suggesting a transition in which, after a rapid growth corresponding to an increase in fluence and number of excited modes (appearing on a smooth fluorescence spectrum), S reaches a maximum (RFRL regime), followed by the spectrum becoming smoother as Θ grows until an IFRL-like emission is achieved (Fig. 2c). Note that smoothing at high Θ is not due to averaging, because sharp peaks are also absent in the single shot spectra.

Parameter Θ also affects the inter-mode spectral correlation. In Fig. 3c we show that intensities for a random pair of peaks of an RFRL pumping configuration ($\Theta = 18°$, average spectra reported in Fig. 3a) obtained for 100 shots are uncorrelated. For $\Theta = 360°$ the subtle features present on top of the otherwise smooth spectrum (Fig. 3b) are repeatable from shot to shot (thus characteristic of the cluster considered) and show strongly correlated intensities (Fig. 3d). Figure 3e shows the average Pearson correlation C (see Supplementary Information) obtained from all possible pairs among the 15 most intense peaks (105 pairs) versus Θ for sample C1. The onset of a strongly correlated regime is obtained for $\Theta \cong 120°$. The same transition was observed in all samples considered, revealing a universal trend in which $C \cong 1$ when $\Theta > 180°$. Further measurements (see Supplementary Information) allow us to exclude artefacts from spontaneous emission or from intensity fluctuations.

In previous experiments on RFRL, a tightly focused pump spot was used to excite a limited number of modes, thus obtaining a spectral emission displaying narrow spikes[17,22]. In our approach, for small Θ, we select modes that are strongly coupled with a directional input but dwell at distant positions (Fig. 1c–e). In the absence of spatial overlap their mutual interaction is negligible, and the spectra obtained feature narrow peaks with limited correlation (Fig. 3e for low Θ). Conversely, when we excite a large number of spatially overlapped resonances, this results in a strongly correlated emission (Fig. 3e for large Θ) and a spatially uniform intensity distribution without hot spots (Fig. 1f) due to pronounced interaction between the modes. The increased degree of interaction is also con- Q6 firmed by time-resolved measurement of the RL emission[23] (Supplementary Fig. 5). We find that the emitted pulse is indeed affected by Θ, being shortened by $\sim$30% in the strongly correlated regime compared with the uncorrelated regime.

We reproduced these results within the framework of coupled mode theory (CMT[1,11,12]) by considering a set of $N = 50$ modes at different frequencies[24], subject to mode repulsion[25,26] and excited in random initial conditions by an external pump pulse (see Supplementary Information). In our model the role of Θ is played by the variable $2 \times n_c$, that is, the number of resonances to which every mode couples.

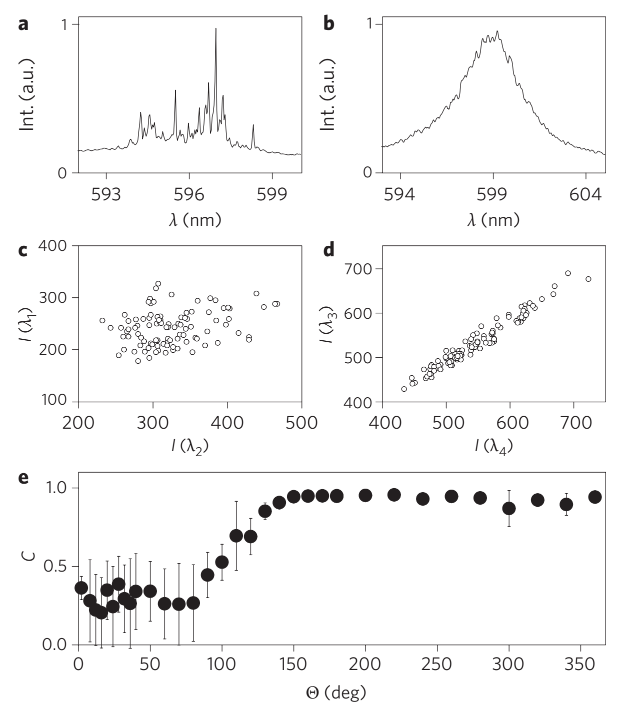

Figure 3 | Onset of a correlated random laser. a,**b**, Normalized average spectra from cluster C1 for $\Theta = 18°$ and $\Theta = 360°$, respectively. **c**, Intensity values of the modes at wavelengths $\lambda_1 = 597.2$ nm and $\lambda_2 = 596.7$ nm obtained for 100 single shots in the pumping configuration with $\Theta = 18°$. **d**, As in **c**, but for wavelengths $\lambda_3 = 598.4$ nm and $\lambda_4 = 598.7$ nm with $\Theta = 360°$. **e**, Correlation C averaged over all possible combinations of the 15 most intense peaks versus Θ. Error bars represent statistical errors from all 105 pairs. Q14

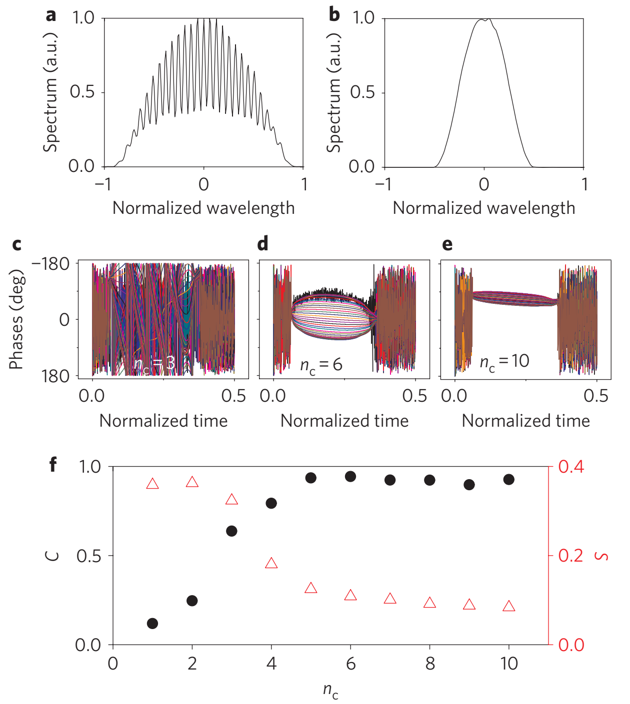

Figure 4 | Results from numerical CMT calculations. a,b, Spectra obtained from 50 modes for $n_c = 0$ and $n_c = 10$, respectively. **c–e**, Phases plotted versus time for $n_c = 3$, $n_c = 6$ and $n_c = 10$. **f**, Numerically calculated C Q7 (filled circles) and S (open triangles) as a function of n_c.

Figure 4 reports the result of our CMT calculations. Figure 4a presents average spectra for $n_c = 0$, showing sharp peaks and resembling an RFRL. Figure 4b shows the same for $n_c = 10$, for which an IFRL-like emission is retrieved that includes small features on top. The difference between the two regimes becomes manifest in the time evolution of the modes. The phases of the 50 weakly coupled modes ($n_c = 3$, Fig. 4c) oscillate uncorrelated, but begin to synchronize as the coupling increases (Fig. 4d, $n_c = 6$). Finally, the mode-locked regime is found for $n_c = 10$ (Fig. 4e). Note that the phases are significant only in the time window where the pump pulse is present (range [0.1,0.4] in the figure; for details see Supplementary Information). The numerically retrieved collective parameters C and S (reported in Fig. 4f as filled circles and open triangles, respect- Q7 ively, as a function of n_c) agree with the experimental results.

In conclusion, by using a pumping scheme that enables the selection of the number of activated modes in a random laser, we demonstrate that RLs may be prepared in two distinct regimes by controlling the shape of the pump. When pumping is nearly unidirectional, few (barely interacting) modes are turned on and appear as sharp, uncorrelated peaks in the spectrum. By increasing the angular span of the Q8 pump spot, many resonances intervene, generating a smooth emission spectrum with a high degree of correlation, and shorter lifetime. All the phenomena reported can be accounted for by assuming a phase-locking transition, the direct proof of which requires measurement of the time evolution of the phases of the modes, which is beyond Q9 the current state of the art. By unveiling the intimate and unique nature of random lasers, these experiments pave the way for a new generation of miniaturized optical devices with engineered and tunable spectral emission, and also lay the foundations for a bridge between disordered photonics and the statistical physics of complex systems.

Methods

Stripe pumping. A stripe-shaped pumped area with a length of 1.6 mm (Fig. 1a) and width of 16 μm was used to obtain a quasi-one-dimensional area to act as a strongly directional source with the cluster located at the centre of the stripe.

Pie pumping. To control the directions from which stimulated emission fed the modes, we designed 'pie shaped pumping'. The excited area consisted of a disk (diameter, 150 μm) centred on the cluster (to assure homogeneous pumping even to the largest clusters) to which two symmetrical wedges of much larger radius (diameter, 1 mm) and controllable orientation and aperture angle ($\Theta/2$) were added, serving as launch pad for directional stimulated emission. A single wedge configuration led to the same results, but proved to be hydrodynamically less stable. The central circle placed the cluster barely below the lasing threshold, preparing the system for lasing once the wedges were turned on. The angular aperture Θ controlled the angular aperture with which stimulated emission was produced and therefore controlled the number of modes expected to be excited.

Spikiness. To classify a RL into the IFRL or RFRL categories we analysed the Fourier transform power spectrum (FTS) of the emission. S is defined as the high-frequency fraction of the total FTS area, that is, the spectral power above a frequency threshold. As a cutoff we defined $K = 1.20\ \mathrm{nm}^{-1}$ in the horizontal scale of the FTS, then calculated S as the area of the FTS lying in the high period part from K Q10 (corresponding to periods greater than K). S returns a value close to one for very spiky spectra, and a value close to 0 for smooth spectra.

Received 10 April 2011; accepted 2 August 2011; published online XX XX 2011

References

1. Haus, H. Mode-locking of lasers. *IEEE J. Sel. Top. Quantum Electron.* **6,** 1173–1185 (2000).
2. Kutz, J. N. Mode-locked soliton lasers. *SIAM Rev.* **48,** 629–678 (2006).
3. Wiersma, D. S. The physics and applications of random lasers. *Nature Phys.* **4,** 359–367 (2008).
4. Cao, H. *et al.* Random laser action in semiconductor powder. *Phys. Rev. Lett.* **82,** 2278–2281 (1999).
5. van der Molen, K. L., Tjerkstra, R. W., Mosk, A. P. & Lagendijk, A. Spatial extent of random laser modes. *Phys. Rev. Lett.* **98,** 143901 (2007).
6. Letokhov, V. Generation of light by a scattering medium with negative resonance absorption. *Zh. Eksp. Teor. Fiz.* **53,** 1442–1447 (1967).
7. Lawandy, N. M., Balachandran, R. M., Gomes, A. S. L. & Sauvain, E. Laser action in strongly scattering media. *Nature* **368,** 436–438 (1994).
8. Froufe-Pérez, L. S., Guerin, W., Carminati, R. & Kaiser, R. Threshold of a random laser with cold atoms. *Phys. Rev. Lett.* **102,** 173903 (2009).
9. Mujumdar, S., Türck, V., Torre, R. & Wiersma, D. S. Chaotic behavior of a random laser with static disorder. *Phys. Rev. A* **76,** 033807 (2007).
10. Lepri, S., Cavalieri, S., Oppo, G.-L. & Wiersma, D. S. Statistical regimes of random laser fluctuations. *Phys. Rev. A* **75,** 063820 (2007).
11. Leuzzi, L., Conti, C., Folli, V., Angelani, L. & Ruocco, G. Phase diagram and complexity of mode-locked lasers: from order to disorder. *Phys. Rev. Lett.* **102,** 083901 (2009).
12. Conti, C., Leonetti, M., Fratalocchi, A., Angelani, L. & Ruocco, G. Condensation in disordered lasers: theory, $3d+1$ simulations, and experiments. *Phys. Rev. Lett.* **101,** 143901 (2008).
13. Gouedard, C., Husson, D., Sauteret, C., Auzel, F. & Migus, A. Generation of spatially incoherent short pulses in laser-pumped neodymium stoichiometric crystals and powders. *J. Opt. Soc. Am. B* **10,** 2358–2363 (1993).
14. Wiersma, D. S. & Lagendijk, A. Light diffusion with gain and random lasers. *Phys. Rev. E* **54,** 4256–4265 (1996).
15. van der Molen, K. L., Mosk, A. P. & Lagendijk, A. Quantitative analysis of several random lasers. *Opt. Commun.* **278,** 110–113 (2007).
16. Conti, C. & Fratalocchi, A. Dynamic light diffusion, Anderson localization and lasing in disordered inverted opals: 3*d ab-initio* Maxwell–Bloch computation. *Nature Phys.* **4,** 794 (2008). Q11
17. Cao, H. *et al.* Spatial confinement of laser light in active random media. *Phys. Rev. Lett.* **84,** 5584–5587 (2000).
18. Fallert, J. *et al.* Co-existence of strongly and weakly localized random laser modes. *Nature Photon.* **3,** 279–282 (2009).
19. Tureci, H. E., Ge, L., Rotter, S. & Stone, A. D. Strong interactions in multimode random lasers. *Science* **320,** 643 (2008). Q11
20. Gordon, A. & Fischer, B. Phase transition theory of many-mode ordering and pulse formation in lasers. *Phys. Rev. Lett.* **89,** 103901 (2002).
21. Picozzi, A. & Haelterman, M. Condensation in Hamiltonian parametric wave interaction. *Phys. Rev. Lett.* **92,** 103901 (2004).
22. El-Dardiry, R. G. S., Mosk, A. P., Muskens, O. L. & Lagendijk, A. Experimental studies on the mode structure of random lasers. *Phys. Rev. A* **81,** 043830 (2010).
23. Siddique, M., Alfano, R. R., Berger, G. A., Kempe, M. & Genack, A. Z. Time-resolved studies of stimulated emission from colloidal dye solutions. *Opt. Lett.* **21,** 450–452 (1996).
24. Chabanov, A. A., Zhang, Z. Q. & Genack, A. Z. Breakdown of diffusion in dynamics of extended waves in mesoscopic media. *Phys. Rev. Lett.* **90,** 203903 (2003).

25. Cao, H., Jiang, X., Ling, Y., Xu, J. Y. & Soukoulis, C. M. Mode repulsion and mode coupling in random lasers. *Phys. Rev. B* **67,** 161101 (2003).
26. van der Molen, K. L., Tjerkstra, R. W., Mosk, A. P. & Lagendijk, A. Spatial extent of random laser modes. *Phys. Rev. Lett.* **98,** 143901 (2007).

Acknowledgements

This work was supported by ERC grant FP7/2007-2013 no. 201766 CINECA; EU FP7 NoE Nanophotonics4Enery grant no. 248855; the Spanish MICINN CSD2007-0046 (Nanolight.es); MAT2009-07841 (GLUSFA) and Comunidad de Madrid S2009/MAT-1756 (PHAMA).

Author contributions

All authors contributed equally to the work presented in this Letter.

Additional information

The authors declare no competing financial interests. Supplementary information accompanies this paper at www.nature.com/naturephotonics. Reprints and permission information is available online at http://www.nature.com/reprints. Correspondence and requests for materials should be addressed to C.L.